Report C87A-25



# ADVANCED DOUBLE LAYER CAPACITOR

Prepared by:

Anthony B. LaConti, Ph.D.
Philip Lessner, Ph.D.
S. Sarangapani, Ph.D.



**GINER, INC.**
14 Spring Street
Waltham, MA 02254-9147
(617) 899-7270

January, 1990

6th Quarter Interim Technical Report

August 1, 1989 to October 31, 1989

Contract No. N00014-88-C-0391
ARPA Order No. 9526

Prepared For:

**OFFICE OF NAVAL RESEARCH**
Department of the Navy
800 N. Quincy Street
Arlington, Virginia 22217

*The views and conclusions contained in this document are those of the authors and should not be interpreted as necessarily representing the official policies, either expressed or implied, of the Defense Advanced Research Projects Agency or the U.S. Government.*

**THIS DOCUMENT HAS BEEN APPROVED FOR PUBLIC RELEASE AND SALE. ITS DISTRIBUTION IS UNLIMITED ~~WITH THE EXCEPTION OF THE APPENDIX WHICH IS LIMITED TO GOVERNMENT PERSONNEL.~~**

## TABLE OF CONTENTS






GINER, INC. 14 SPRING STREET • WALTHAM, MASSACHUSETTS 02254-9147 • (617) 899-7270

## LIST OF TABLES AND FIGURES








GINER, INC.

14 SPRING STREET • WALTHAM, MASSACHUSETTS 02254-9147 • (617) 899-7270

## 1. TECHNICAL OBJECTIVES

The overall goal of this project is to develop electrochemical capacitors utilizing a solid ionomer electrolyte. An advantage of these devices over conventional double layer capacitors would be the absence of free liquid electrolyte and thus greater safety and reliability.

In the sixth quarter, we concentrated our efforts in three areas: 1) preparation and characterization of electrode materials, 2) preparation of membrane and electrode (M and E) assemblies that have high capacitance and minimum internal resistance, and 3) development of cell hardware that can contain the M and E for extended periods of time without loss of water and contributes negligibly to the total internal resistance.

## 2. EXPERIMENTAL METHODS

### 2.1 Preparation and Characterization of Electrode Materials

#### 2.1.1 Preparation

$RuO_x$ was prepared by thermal treatment of $RuCl_3$-$NaNO_3$ for three hours at 500°C followed by rapid quenching in water. The powder was washed until free of chloride (by the $AgNO_3$ test) and then centrifuged to collect the $RuO_x$ particulates.

#### 2.1.2 Particle Size Analysis

A sample of $RuO_x$ powder was sent to Micromeritics (Norcross, GA) for particle size analysis by gravity sedimentation. For this type of analyses, particles are allowed to settle slowly in a viscous medium. X-Ray absorption is used to determine the concentration of particles at each depth in the liquid. Stoke's law is used to calculate the equivalent spherical diameter of the particles at each depth in the liquid.

#### 2.1.3 Nitrogen Porosimetry

A sample of $RuO_x$ was sent to Micromeritics for determination of surface area (by the multipoint BET method), pore volume, and pore size distribution (by the BJH method).



GINER, INC. 14 SPRING STREET • WALTHAM, MASSACHUSETTS 02254-9147 • (617) 899-7270

## 2.2 Preparation of M and Es

Prior to this quarter, the M and E preparation procedure had evolved from painting the $RuO_x$ mixture directly on the membrane to a modified Giner, Inc. proprietary method. During this reporting period, further optimization of M and E fabrication methods were made to improve quality and enhance the electrochemical capacitance of the $RuO_2$ electrode structures.

The modified Giner, Inc. method involves bonding the $RuO_x$-Nafion composite directly to a carbon-Ti screen current collector. The carbons used and typical fabrication parameters are listed in **Table I.** Black Pearls (Cabot Corporation) was chosen because it is a high surface area (1000 $m^2/g$) and highly conductive carbon black. Heat treatments lower the surface area (to about 250 $m^2/g$) and the heat treated material requires less Teflon to make a mechanically stable electrode. PANEX is a carbon paper; it is lightly Teflonized for mechanical stability. Vulcan XC-72 (Cabot Corporation) is a conductive carbon black of surface area 250 $m^2/g$.

**Table I: Current Collector - Backing Layers**

| Type | Loading ($mg/cm^2$) | Teflon (%) |
|---|---|---|
| Black Pearls | 5 | 25 |
| Heat-Treated Black Pearls | 10 | 5 |
| PANEX | | |
| Vulcan XC-72/PANEX | 10 | 40 |

## 2.3 Cell Hardware

During the 5th Quarter, sealed cell hardware with polymeric endplates and an O-ring was developed. This hardware continued to be used during the 6th Quarter. We have also developed hardware based on metallic endplates and fluoropolymer gasketing. An exploded view of this hardware is shown in **Figure 1.** The endplates are machined from titanium metal (0.125" thick). Each plate is lightly platinum plated (0.5 to 1 $mg/cm^2$) in the area that contacts the M and E current collector. A fluoropolymer gasket (TFE or FEP) of appropriate thickness is placed around the M and E. The plates are compressed against the M and E and gasket using insulated metal bolts. Contact to the external circuit is via gold-plated tabs.

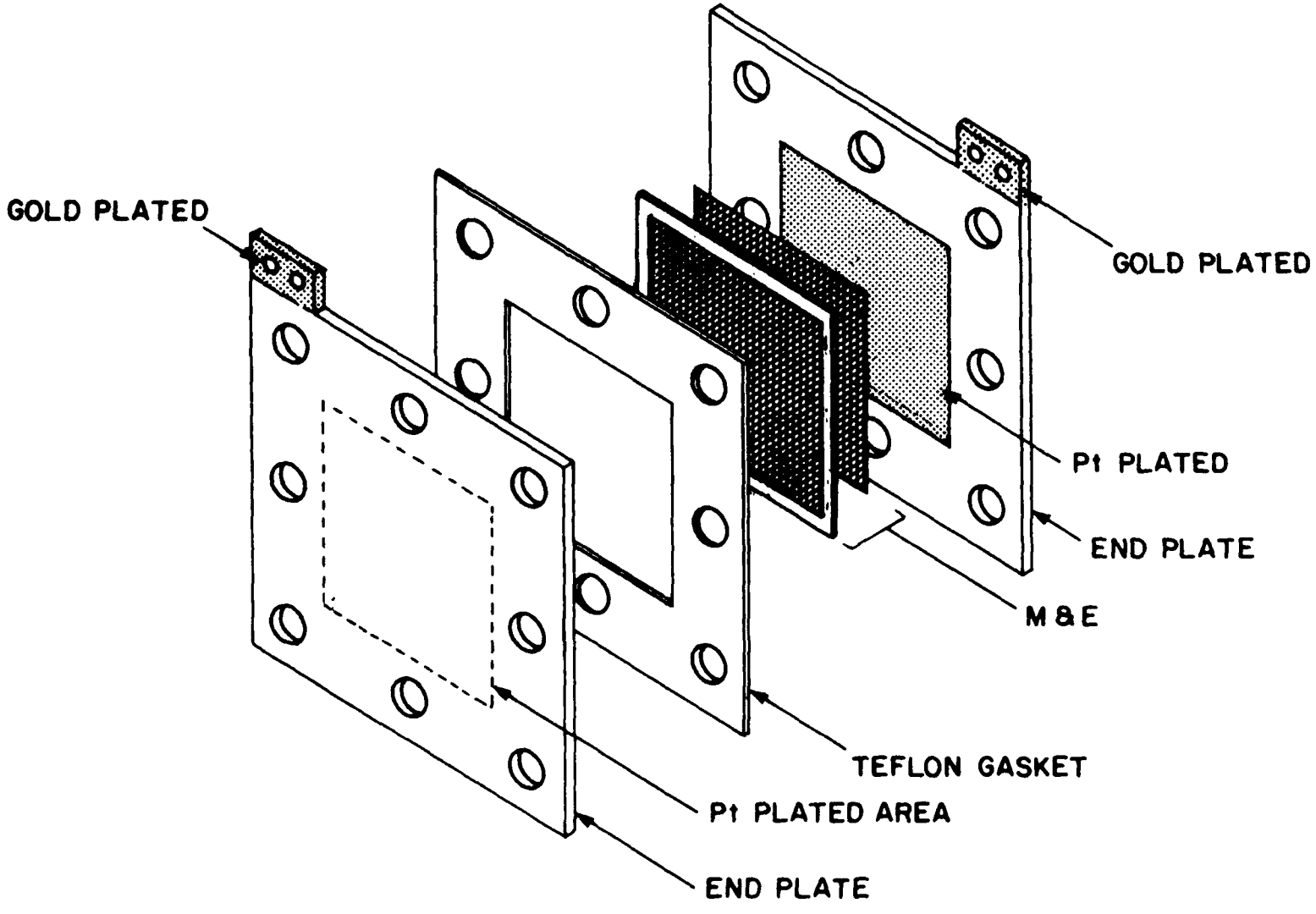


Figure 1: Exploded View of Capacitor Cell Hardware with Titanium End Plates

### 2.4 Cell Testing

Cells were tested for capacitance by discharge through a resistive load. Current interruption was used to measure internal resistance. The equipment and procedures for these tests have been described in the 5th Quarterly Report.

## 3. RESULTS AND DISCUSSION

### 3.1 Electrode Materials

**Figure 2** shows the particle size distribution expressed as mass % in an interval vs. particle diameter. Most of the particle mass is in the 5 to 10 μm diameter interval. The median diameter based on the mass distribution is 5.52 μm. The median diameter based on the number distribution is 0.42 μm. These results of particle size analysis by gravity sedimentation are in agreement with those measured by computerized particle counting on the SEM.

TEM observation showed that the size of the individual crystallites was on the order of 0.02 μm. These crystallites are aggregated into porous particles with sizes ranging from the submicron to several tens of microns (particles of diameter greater than about 40 μm were removed by sieving). The size range of the porous aggregates is due to either the precursor ($RuCl_3$) morphology or sintering of crystallites during transformation.

A multipoint BET analyses was done on this sample to check the validity of the BET isotherm for $RuO_x$ and to check the assumptions of the single point method. **Figure 3** is a plot of $1/[V(P_o/P-1)]$ vs. $P/P_o$. If the BET equation:

$$\frac{1}{C[P_o/P-1]} = \frac{1}{V_mC} + [(C-1)/V_mC]\ \frac{P}{P_o}$$

is obeyed, then this plot should be a straight line with an intercept of $V_mC$ and a slope of $[(C-1)/V_mC]$. Figure 3 shows that a straight line is obtained; and, therefore, the BET equation is obeyed. From the plot a surface area of 103.26 $m^2/g$ is obtained. Solving for $V_m$ and C gives $V_m$ = 23.72 $cm^2/g$ (STP) and C = 91.23. If C >> 1, then the single point BET surface area should be a good approximation. The single point surface area is 100.59 $m^2/g$ which is within 2.6% of the multipoint surface area.


GINER, INC. 14 SPRING STREET • WALTHAM, MASSACHUSETTS 02254-9147 • (617) 899-7270

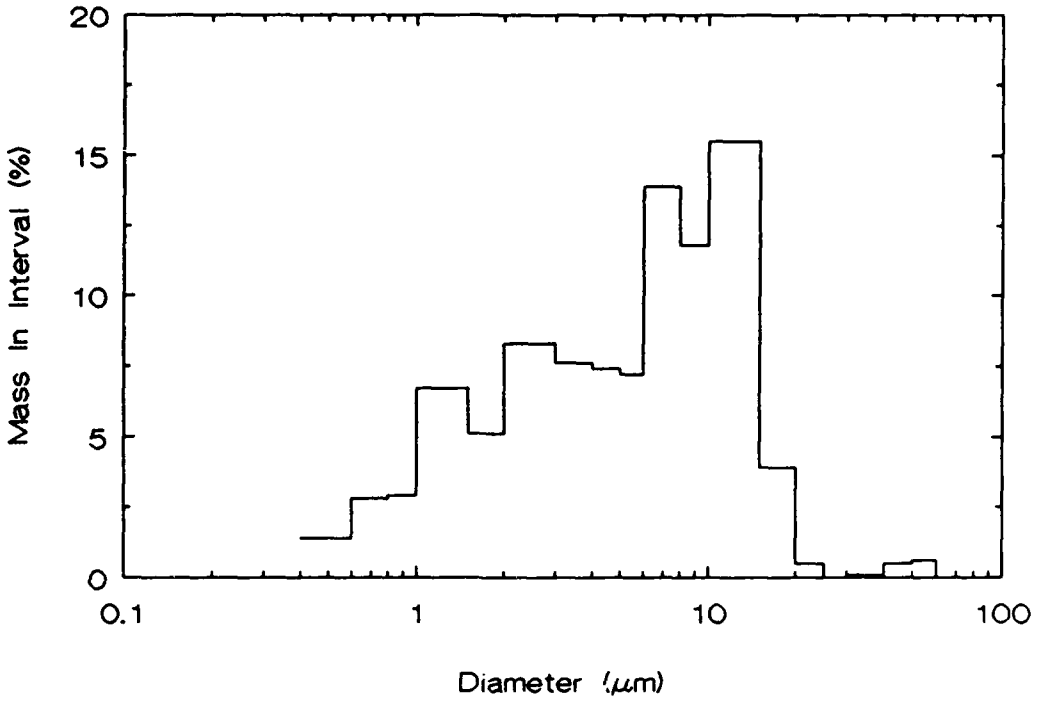


**Figure 2: Mass Distribution of $RuO_x$ Particulates Measured by Gravity Sedimentation**

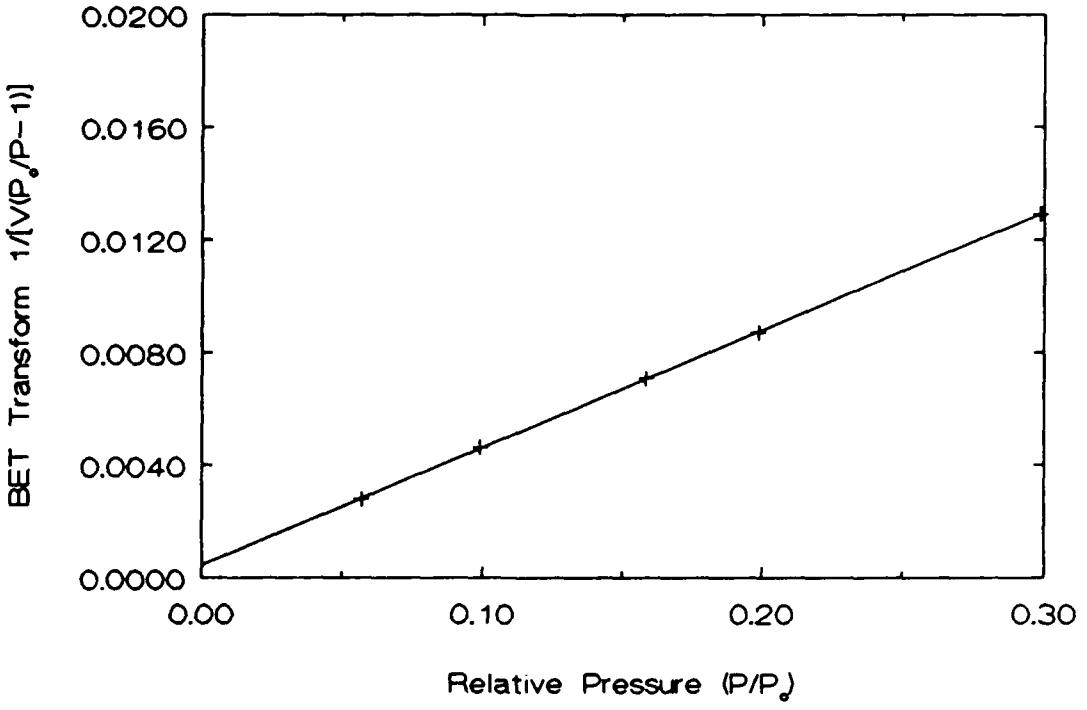


**Figure 3: BET Transform vs. Relative Pressure for Nitrogen Adsorption on $RuO_x$**

The total pore volume and pore size distribution were measured by the method of Barrett, Joyner, and Halenda (BJH method). **Figure 4** is a plot of pore volume vs. pore diameter. The size range of pores accessible by nitrogen porosimetry is 17 to 3000 Å. The volume of pores in this range is 0.260 $cm^3/g$. This is close to the 0.258 $cm^3/g$ measured by mercury porosimetry (30 Å to 120 μm diameter range) and is close to the 0.235 $cm^3/g$ measured by Balko, et al. (1980) for $RuO_x$ similarly prepared.

**Figure 5** is a plot of cumulative surface area vs. pore diameter. The surface area in pores greater than 200 Å in diameter is less than 10 $m^2/g$. Most of the surface area is in pores less than 100 Å in diameter. The average pore diameter is about 100 Å.

The morphology of porous aggregates of $RuO_x$ crystallites is expected from the synthesis of a dense material (6.67 $g/cm^2$ for $RuO_x$) from a less dense material (3.11 $g/cm^3$ for $RuCl_3$). The measured pore volume of 0.26 $cm^2/g$ is about 30% greater than the difference in specific volumes of the two materials of 0.18 $cm^3/g$. Oxides, when synthesized from their corresponding hydroxides, have pore volumes close to (or less when pores are closed off) the difference in specific volume between the precursor of the product. This means that the transformation is more complex than a simple pseudomorphic, topotatic transformation. This is not surprising because the transformation of $RuCl_3$ into $RuO_x$ involves the incorporation of oxygen into the lattice and a change in oxidation state.

In order to make use of the surface area of the $RuO_x$ electrode material, the electrolyte must penetrate into the pores. Small electrolytes such as $H_2SO_4$ and associated water molecules have effective diameters of less than 20 Å and could effectively contact all of the surface area of the $RuO_x$ porous aggregates. The 1100 EW Nafion electrolyte is much larger; an effective size of over 200 Å has been reported for the solubilized form (Aldebert, et al., 1986). The Nafion electrolyte may not be able to penetrate into the $RuO_x$ pores. This is the same conclusion as reached in the 4th Quarterly Report on the basis of the mercury porosimetry results.


GINER, INC. 14 SPRING STREET • WALTHAM, MASSACHUSETTS 02254-9147 • (617) 899-7270

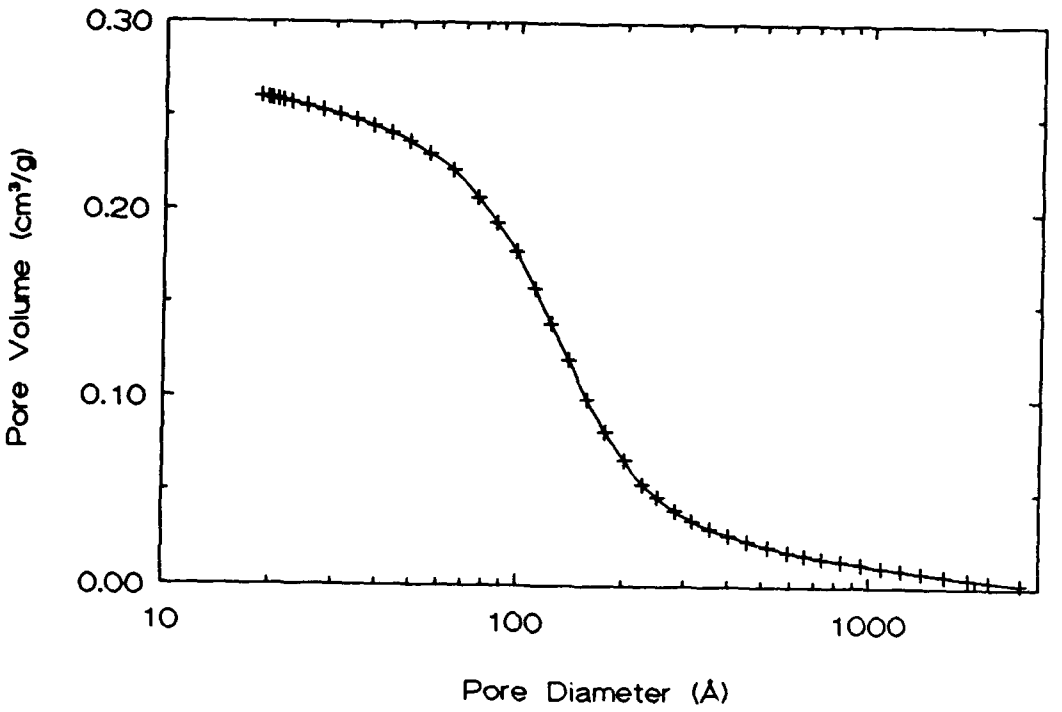


**Figure 4: Cumulative Pore Volume vs. Pore Diameter for $RuO_x$ Prepared by the Thermal Method**

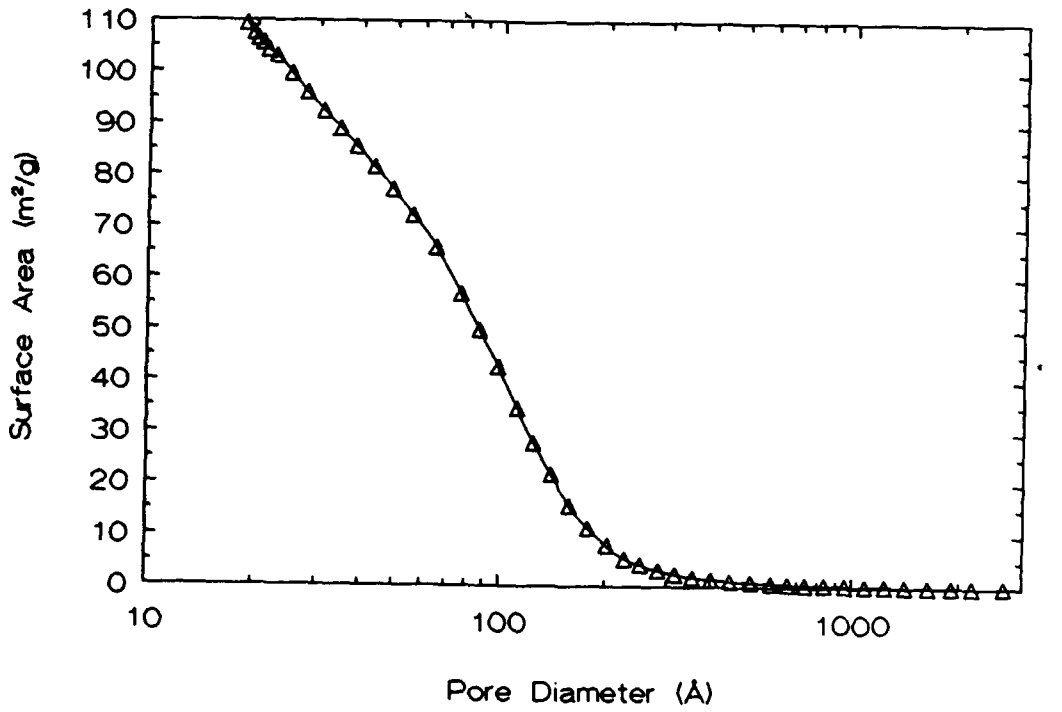


**Figure 5: Cumulative Surface Area vs. Pore Diameter for $RuO_x$ Prepared by the Thermal Method**

## 3.2 Cell Testing

### 3.2.1 Capacitance

Capacitance of the M and Es made on the different backing layers, using the modified Giner, Inc. proprietary method, was measured by charging the M and E, discharging through at 10 ohm resistor, and dividing the total charge by the initial voltage (see the 5th Quarterly Report for a derivation) to obtain the capacitance. **Table II** lists the measured capacitances. M and Es fabricated using the $RuO_x$-Nafion mixture on Black Pearls carbon had significantly higher capacitance than those saturated with PANEX or Vulcan XC-72 backings. When Nafion 111 (0.001 inch thick) or a Dow membrane was substituted for the standard Nafion 117 membrane, the capacitance remained greater than 1 F/cm². A control M and E with Black Pearls electrodes painted with Nafion, but with no $RuO_x$ had a capacitance of only 0.16 F/cm². Therefore, the $RuO_x$ layer makes a significant contribution to the capacitance of the M and E. Heat treated Black Pearls also gave an M and E with high capacitance but not as high as plain Black Pearls.

**Table II: Capacitance of M and Es Discharging Through a 10-ohm Resistor**

| M and E | Backing Layer | $RuO_x$ Loading (mg/cm²) | Membrane | Capacitance (F/cm²) |
|---|---|---|---|---|
| 369-62-1 | Black Pearls | 15,20 | Nafion 117 | 1.20 |
| 369-69-1 | Black Pearls | 15,15 | Nafion 117 | 0.57 |
| 377-32-1 | Black Pearls | 19.5,22.3 | Nafion 117 | 1.15 |
| 377-32-5 | Black Pearls | 15,16.5 | Nafion 117 | 1.33 |
| 369-92-1 | Black Pearls | 16.5,17 | Nafion 111 | 1.17 |
| 377-38-4 | Black Pearls | 15,18.4 | Dow | 1.13 |
| 369-64-1 | Black Pearls | 0,0 | Nafion 117 | 0.16 |
| 377-49-1 | HT Black Pearls | 13.3,18 | Nafion 117 | 0.84 |
| 69-63-1 | PANEX | | Nafion 117 | 0.59 |
| 69-65-1 | PANEX | 10,12 | Nafion 117 | 0.46 |
| 369-66-1 | Vulcan XC-72 /PANEX | 15,15 | Nafion 117 | 0.57 |
| 369-65-2 | Black Pearls+ | 20,20 | Nafion 117 | 0.90 |
| 369-65-3 | Black Pearls* | 15,15 | Nafion 117 | 0.58 |

+ slurry cast * with Ru black layer on membrane

The origin of the higher capacitances of the Black Pearls M and Es is not well understood at this time. One idea that can be advanced is that painting on the Black Pearls carbon allows a

better dispersion of $RuO_x$ aggregates and, therefore, better contact between the $RuO_x$ and Nafion is achieved. This would be especially true if, as postulated in the previous section, the Nafion coats the outside of the porous aggregates and does not penetrate significantly into their interior.

Another area requiring explanation is the magnitude of the capacitances obtained with the M and Es. If we assume that the $RuO_x$ powder has a surface area of 100 $m^2/g$ and the electrode loading is 15 $mg/cm^2$, then the electrode roughness factor is 15,000. The double layer and pseudo capacitance on $RuO_x$ is on the order of 150 $\mu F/real\ cm^2$ (Kleijn and Lyklema, 1987). This means the capacitance per electrode should be 2.25 $F/geo\text{-}cm^2$ or per M and E 1.125 $F/geo\text{-}cm^2$ (two electrodes in series). Since this is near the capacitances measured, either the surfaces of the pores of the $RuO_x$ can charge up or bulk $RuO_x$ is being utilized in charge storage. Both these explanations are consistent with the multiple time constants inferred from the AC impedance and resistive load discharge experiments reported previously.

### 3.2.2 Internal Resistance

The internal resistance of the cell (or cell stack) will ultimately limit the rate at which power can be delivered. Consider the circuit given in **Figure 6**. Here the device is considered to be a capacitor with capacitance C and internal resistance $R_i$. It discharges through a load with resistance $R_L$. The total resistance $R_t$ is the sum of $R_i$ and $R_L$. The power delivered to the load is the product of current and voltage:

$$P = iV = \frac{V_o^2 R_L}{R_t^2} \exp(-2t/R_tC)$$

This can be integrated to give the energy delivered to the load after a time $t_p$:

$$E_L = \frac{1}{2} V_o^2 C \frac{R_L}{R_t} [1-\exp(-2t_p/R_tC)]$$

This equation demonstrates that the energy delivered in time $t_p$ will be decreased due to $R_t$ being greater than $R_L$.



GINER, INC. 14 SPRING STREET • WALTHAM, MASSACHUSETTS 02254-9147 • (617) 899-7270

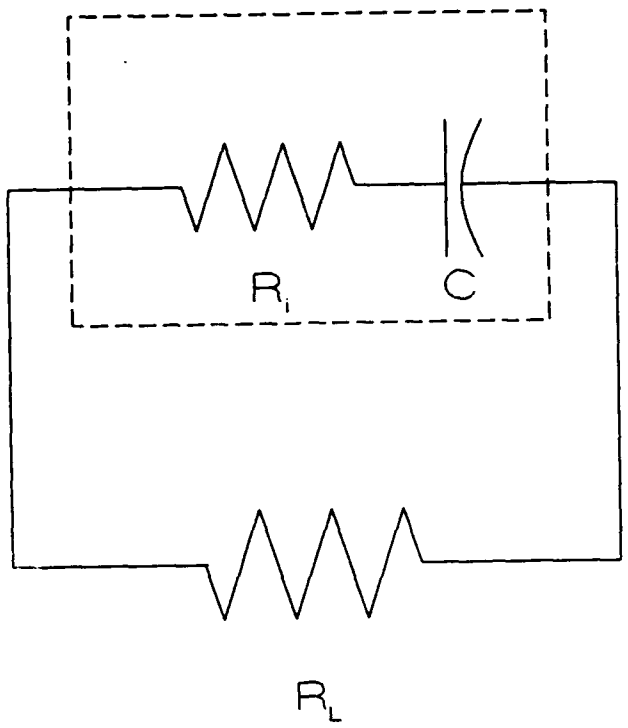


**Figure 6: Equivalent Circuit of a Capacitor with Capacitance, C, and Internal Resistance, $R_i$, Discharging Across a Load Resistance, $R_L$**

As a hypothetical example, consider the case where C = 0.33F, $V_o$ = 8V, $R_L$ = 1 ohm and $t_p$ = 1 sec. The DC energy storage of this capacitor is 10J and 9.98J can be delivered to this load in 1 second if $R_i$ = 0. **Figure 7** shows how the energy delivered to the load declines with increasing internal resistance. With a 100 mΩ internal resistance only 9.06 J can be delivered, and if the internal resistance is doubled to 200 mΩ then only 8.29 J can be delivered.

**Table III** lists the resistance of some M and Es made during this quarter. The acrylic cell hardware (Figure 1 of the 3rd Quarterly Report) was used to hold the M and Es and current interruption was used to measure the resistance. The resistance of an M and E with a Nafion 117 membrane (178 μm thick) is 0.375 ohm-cm². The membrane resistance (for a membrane equilibrated at 100°C with water) should be 0.22 ohm-cm² at 25°C. The resistance of the M and E with the Nafion 111 membrane (25.4 μm thick) is 0.275 ohm-cm² which is far from the factor of seven reduction expected if the electrolyte resistance is the controlling factor.


GINER, INC. 14 SPRING STREET • WALTHAM, MASSACHUSETTS 02254-9147 • (617) 899-7270

GINER, INC.
14 SPRING STREET • WALTHAM, MASSACHUSETTS 02254-9147 • (617) 899-7270



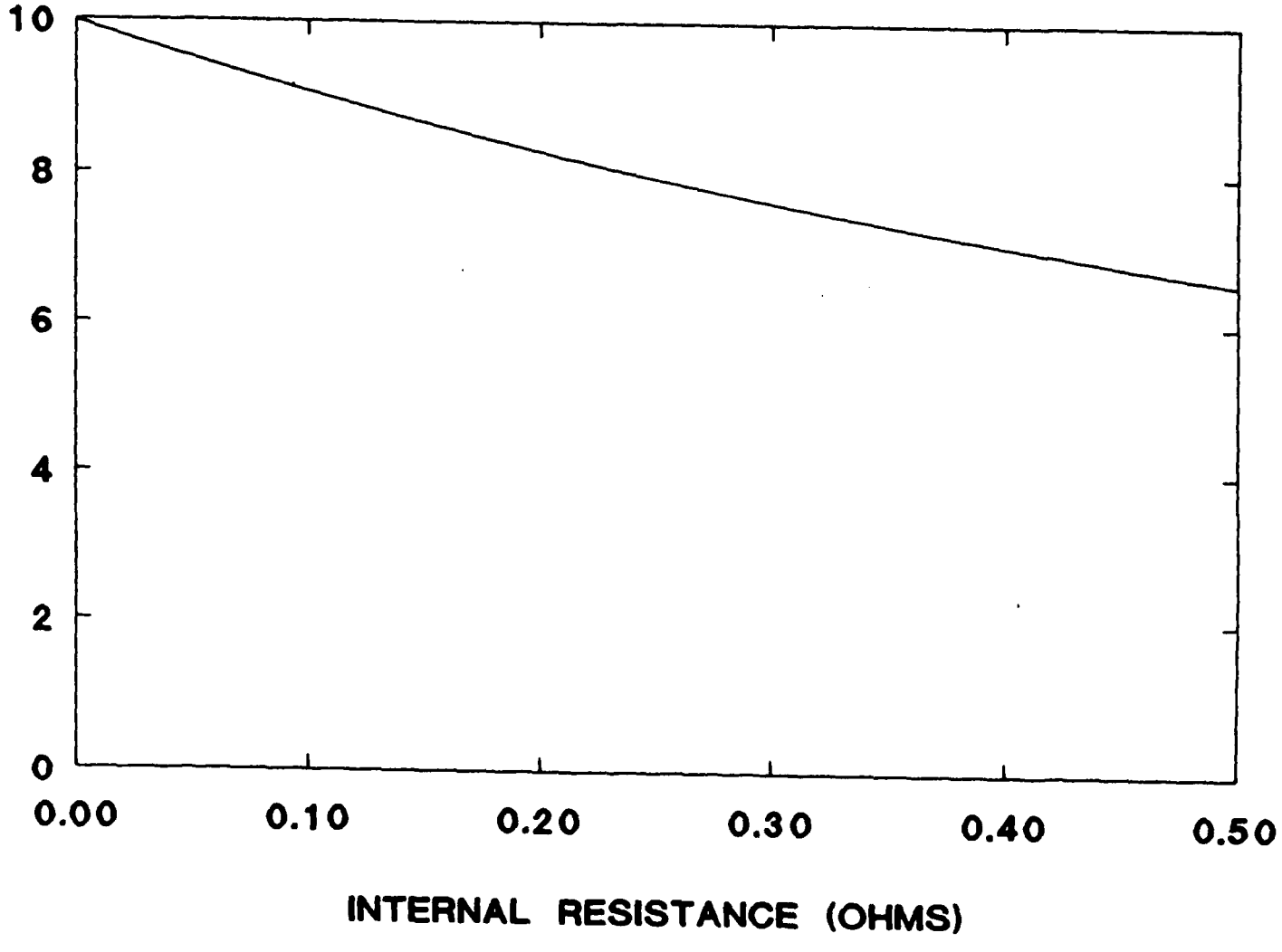


Figure 7: Energy Delivered vs. Internal Resistance for an 8 V, 0.33 F Capacitor

**Table III: Resistance of M and Es**

| M and E | Backing Layer | Membrane | Resistance (ohm/cm²) |
|---|---|---|---|
| 369-32-1 | Black Pearls | Nafion 117 | 0.375 |
| 369-32-5 | Black Pearls | Nafion 117 | 0.375 |
| 377-92-1 | Black Pearls | Nafion 111 | 0.275 |
| 377-38-4 | Black Pearls | Dow | 0.300 |

These results point to other factors other than the electrolyte membrane resistance as contributing to the resistance of the cell. These other resistances can include contact resistances between the electrode and cell plates, contact resistance between the electrode and membrane, and electrode resistance.

### 3.2.3 Long-Term Testing

M and Es were tested for variation in capacitance and internal resistance with time using the cell hardware with polymeric end plates. **Figure 8a** is a plot of internal resistance vs. time for an M and E made by the transfer from metallic foil technique. The higher resistance of the first 20 days is due to using test clips that contributed to the measured resistance. After charging to spade lug connections, the resistance dropped to 0.02 ohms (0.5 ohm-cm²). It has remained stable near that value for over two months demonstrating that loss of water (by membrane dehydration), which would lead to higher resistance, is not taking place. The capacitance (**Figure 8b**) shows somewhat more scatter, but also remains nearby constant with time.

## 4. FUTURE WORK

Cell internal resistance has been identified as a factor that will limit useful power output of the capacitor cells. Studies are being conducted to determine how the different components and component interfaces contribute to the cell internal resistance. Internal resistance and capacitance will also be studied as a function of temperature.

The titanium cell hardware (Figure 1) is an appropriate vehicle for building multi-cell stacks. Multi-cell stacks will be fabricated and evaluated for capacitance, internal resistance and charge retention.


GINER, INC. 14 SPRING STREET • WALTHAM, MASSACHUSETTS 02254-9147 • (617) 899-7270

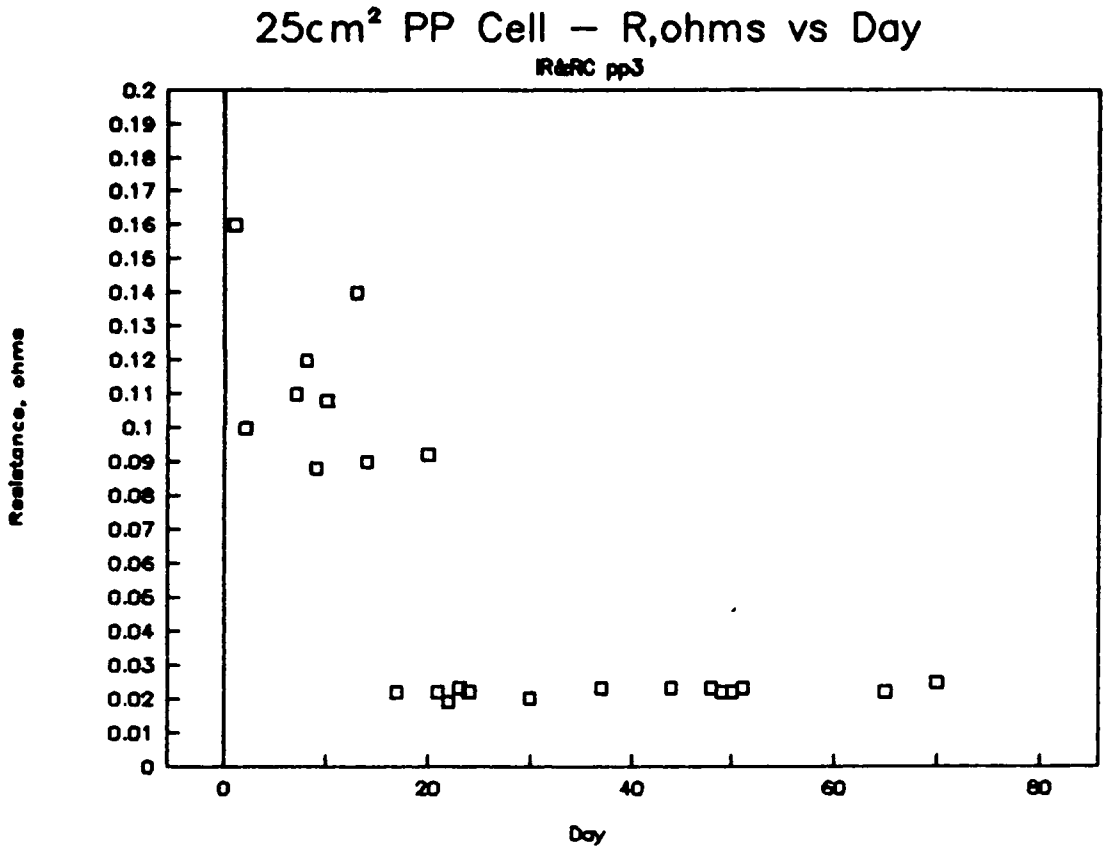


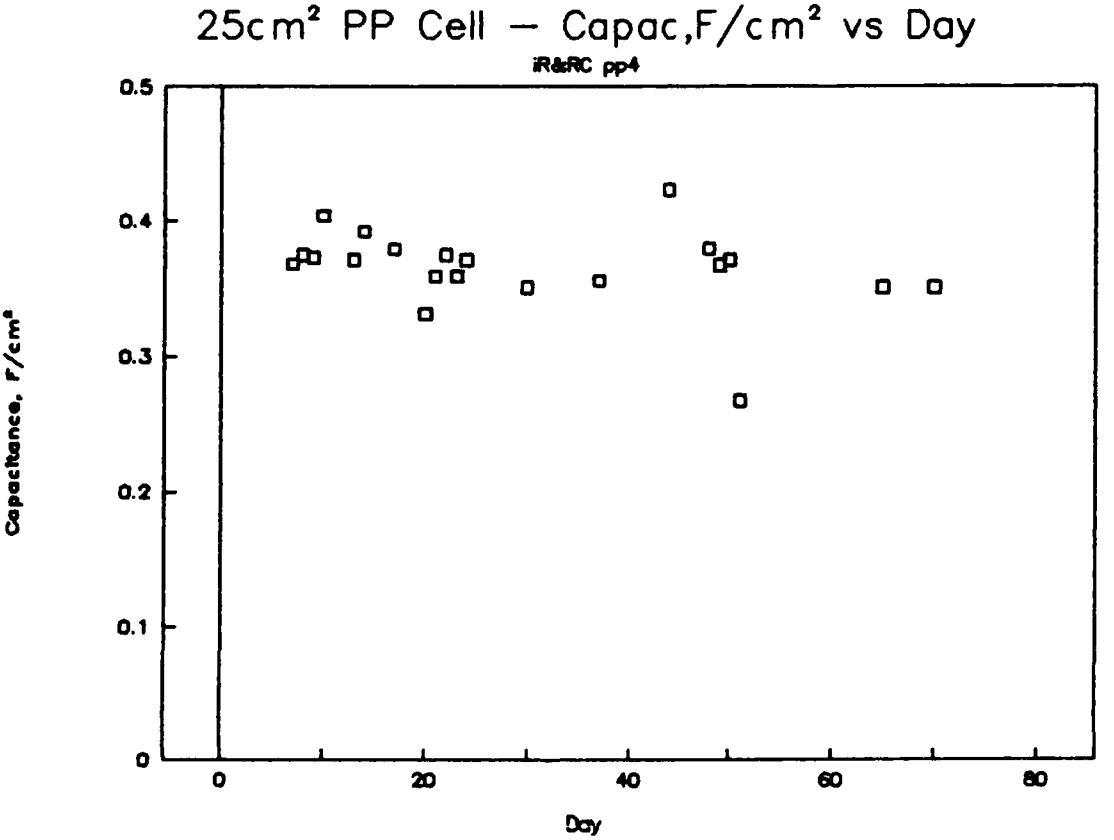


**Figure 8:** **M and E in a 25 cm² Cell with Polypropylene End Plates**
**a) Internal Resistance vs. Time**
**b) Capacitance vs. Time**

## 5. REFERENCES

**Aldebert**, P.B. Dreyfus and M. Pineri, "Small Angle Neutron Scattering of Perfluorosulfonated Ionomers in Solution," *Macromolecules*.

**Balko**, E.N., C.R. Davidson and A.B. Laconti, "Solid Solutions of $RuO_2$ and $IrO_2$," *J. Inorg. Nucl. Chem.*, **42**, 1778 (1980).

**Kleijn**, J.M. and J. Lyklema, "The Electrical Double Layer on Oxides: Specific Adsorption of Chloride and Methylviologen on Ruthenium Dioxide," *J. Colloid and Interface Sci.*, **120**, 511 (1987).